RSC Advances

ROYAL SOCIETY OF CHEMISTRY

www.rsc.org/advances

Polymer coated phosphate glass/hydroxyapatite composite scaffolds for bone tissue engineering applications

R. Govindan[a], G. Suresh Kumar[b] and E.K. Girija*[a]
[a]Department of Physics, Periyar University, Salem 636 011, Tamil Nadu, India.
[b]Department of Physics, K. S. Rangasamy College of Arts and Science (Autonomous), Tiruchengode 637 215, Tamil Nadu, India.

*Corresponding author:
Tel. +91 9444391733; Fax. +91 427 2345124;
E-mail: girijaeaswaradas@gmail.com

ABSTRACT

The development of bioactive ceramic composite scaffold materials with enhanced mechanical strength has been a topic of great interest in bone tissue engineering. In the present study, phosphate glass/hydroxyapatite (PG/HA) composite scaffold with an open-porous structure (~89% porosity and pore size in the range 200−500 μm) has been fabricated by foam replica method. In order to enhance the mechanical strength of this scaffold a polymer coating of alginate, chitosan and gelatin was made on the composite scaffold by immersion method. The polymer coating did not affect the interconnectivity but reduced the porosity of the PG/HA composite scaffold. Biodegradation studies revealed that all the composite scaffolds have undergone significant degradation. But the compressive strength of the gelatin coated scaffold (G-PG/HA) exhibited sevenfold enhancement than the pristine scaffold. The PG/HA and G-PG/HA composite scaffolds revealed excellent biocompatibility with human osteoblast-like MG-63 cells. Hence, G-PG/HA composite scaffold may be a smart promising scaffold for bone tissue engineering.

KEYWORDS: PG/HA composite scaffold, polymer coating, compressive strength, bone tissue engineering

1. INTRODUCTION

It is well documented in the literature that over the last few decades, hundred millions of people across the world are affected by bone related diseases such as joint disease, osteoporosis, spinal disorders, crippling diseases, deformities, *etc*.[1-3] Hence bone replacement is being done widely and implants are needed in many orthopaedic and maxillofacial surgeries. Autografts and allografts have been considered to be the best choices for bone substitutions, since they provide a fast osteointegration with the surrounding tissues after implantation. But, autografts are limited in supply and allografts have the risk of transmitting diseases and can elicit adverse immune reactions. Tissue engineering has become one of the most attractive and alternative approaches for successful regeneration of damaged bone. For bone tissue engineering, bioactive, biocompatible 3D scaffolds with suitable mechanical properties, controlled pore size (100-200 μm) and high porosity (80%) with interconnectivity are the basic requirements.[4-5] In addition scaffold can carry antibiotics and other functionalities such as insulin-like growth factors I and II (IGF-I, IGF-II), transforming growth factors (TGF-beta 1, TGF-beta 2), platelet derived growth factor and bone morphogenetic proteins (BMPs) for efficient bone regeneration.

The porous scaffolds of polymers and bioactive ceramics are being fabricated by various methods such as thermally induced phase separation (TIPS),[6-7] solvent casting,[8-9] particle leaching,[10-11] freeze casting, [12-16] polymer foam replication.[17-21] Among them, polymer foam replication method is capable of yielding porous ceramic structure of required shape which is almost comparable to spongy bone. Also, scaffolds prepared by this method have the advantage of controlling the pore size with interconnected pores. One of the major disadvantages of this method is its poor mechanical strength. However, this disadvantage can be overcome by applying polymer coating which results in a scaffold of ceramic polymer composite that can incorporate the advantages of both. The incorporated polymer phase can fill existing cracks in the structure and thus during fracture a crack bridging mechanism provided by the deformable polymer phase will be active leading to an enhancement of the scaffold toughness, in a similar behavior as collagen fibres increase the fracture toughness of bone.[22-23]

Among the various types of ceramic biomaterials available bioactive and biodegradable ceramics such as calcium phosphates and bioglass® are good choices for bone tissue engineering.

Particularly, glass based biomaterials exhibit better biocompatibility than crystalline phase because an amorphous material has predominant biomineralization.[24] Recently we reported a novel biocompatible, bioactive phosphate glass/hydroxyapatite (PG/HA) nanocomposite as drug carrier for orthopedic applications.[25] Several polymers such as poly (L-lactic) acid (PLLA),[26-27] poly(caprolactone) (PCL),[27] alginate,[27] gelatin,[27-28] and poly-β-hydroxybutyrate[29] have been investigated as possible coating system for bioceramic scaffolds. In general, synthetic polymers exhibit better mechanical strength than natural polymers. However, natural polymers are raw materials that naturally occur in the biological environment[30] and these are biocompatible and enzymatically biodegradable.[31] Drawbacks of synthetic polymers include less predictability of biocompatible, toxic and inflammatory biological response.[32] Natural polymers can provide intrinsic templates for cell adhesion, growth and stimulate an immune response due to their biocompatibility. Also, the microstructures of the natural polymers are highly organized and contain extracellular substance which acts as temporary extracellular matrix (ECM) for successful bone regeneration. Hence, natural polymer coating over the ceramic scaffold is a better approach for making mechanically sound scaffold for orthopedic applications.

From the literature review it is evident that for bone tissue engineering based on ceramic scaffolds such as HA, silicate glass, β-TCP, BCP, borate glass, biosilicate *etc* synthetic polymers like PCL, PLLA, P3HB, natural polymers like alginate, gelatin, chitosan, collagen and combination of synthetic and natural polymers have been investigated by different research groups as coating agent for toughening and drug encapsulation purposes.[33] So far there is no report on natural polymer coating over PG/HA composite scaffold for tissue engineering applications. As a continuation of our previous work on PG/HA nanocomposite we developed a porous scaffold for bone tissue engineering using the PG/HA composite. In the present investigation we attempted to identify a good natural polymer for coating the PG/HA composite scaffold that achieves structural and mechanical stability for bone tissue engineering.

2. MATERIALS AND METHODS

2.1 Preparation of uncoated and polymer coated scaffold

Phosphate glass (PG) of composition $45P_2O_5$-24CaO-$21Na_2O$-5SrO-$5Fe_2O_3$ (mol %) and nano hydroxyapatite (HA) were prepared by melt quenching and microwave irradiation methods[34]

respectively. The ceramic composite scaffold was made with 1:3 ratio of PG and HA composition using polymer foam replication method as described elsewhere.[25] The slurry for scaffold fabrication was prepared by 6 wt% dissolving polyvinyl alcohol (Mw = ~30000, Himedia, India) in water and adding the composite powder with 40 wt% concentration. Polyurethane foam (10 x 10 x10 mm^3) was immersed into the slurry and infiltrated for 1 min. so that the foam struts were coated with bioactive glass particles. The as coated foams were then dried at room temperature overnight and then subjected to a controlled heat treatment. The samples were kept at 400 ºC for 1 h in air to decompose the foam and then at 600 ºC for 2 h to densify the composite.

2.2 Polymer coating on composite scaffold

Polymers such as alginate, gelatin and chitosan were chosen as coating agents to coat the PG/HA composite scaffold. The concentration of alginate and gelatin for coating was adopted from Hum *et al.*[27] as 2% and 5% respectively in aqueous solution. Chitosan concentration was optimized to be 2% in 1.5% glacial acetic acid solution. Coating experiment was performed at room temperature by immersing the pre-wetted ceramic composite scaffold sintered at 600 ºC in the respective polymer solution for 1 min. in the case of alginate and 5 min. for gelatin and chitosan. After immersing in the polymer solution gelatin coating was crosslinked in 0.1% glutaraldehyde solution for 24 h whereas alginate was crosslinked in 100 mM $CaCl_2$ solution for 1 h. Then the PG/HA composite scaffolds were washed in deionized water thrice followed by drying at room temperature for 24 h. The chitosan coated PG/HA composite scaffold was neutralized with 0.1 M NaOH aqueous solution for 30 min., washed with deionized water and dried at 37 ºC. The alginate, chitosan and gelatin coated PG/HA composite scaffolds were named as A-PG/HA composite, C-PG/HA composite and G-PG/HA composite scaffold respectively.

2.3 Characterization of scaffold

The powder X-ray diffraction (PXRD) pattern of the PG, HA and PG/HA composite was recorded using a Rigaku MiniFlex II powder X-ray diffractometer between $10^o \leq 2\theta \leq 60^o$ with Cu Kα monochromatic radiation (1.5406 Å) and the microstructural characterization was carried out by scanning electron microscopy (FEI - QUANTA–FEG 250). The Fourier transform infrared (FTIR) analysis of PG/HA and polymer coated PG/HA composite scaffolds was

performed to identify the functional groups using Bruker Tensor 27 FTIR spectroscopy. Samples were prepared by mixing 1 mg composite powder with 100 mg KBr and pressing into discs and analyzed in the wavenumber range 400–4000 cm^{-1} at a resolution of 4 cm^{-1}.

2.4 Porosity

The density of polymer-coated scaffolds ($\rho_{scaffold}$) was determined from the mass and volume of the PG/HA composite scaffolds before and after coating with polymer. The porosity before (p_1) and after (p_2) coating was calculated using the following equations:

$$p_1 = 1 - \frac{W_1}{\rho_{uncoated} V_1}$$

$$p_2 = 1 - \frac{\left(\frac{W_1}{\rho_{uncoated}} + \frac{W_2 - W_1}{\rho_{polymer}} \right)}{V_2}$$

where W_1, W_2 and V_1, V_2 are the weight and volume of the scaffolds before and after coating respectively; $\rho_{uncoated}$ and $\rho_{polymer}$ are the density of PG/HA composite (2.69 g cm^{-3}) and polymers (gelatin- 1.2 g cm^{-3}, alginate - 1.8 g cm^{-3} and chitosan – 1.34 g cm^{-3})[35-36] respectively. The density of PG/HA composite was calculated by Archimedes principle.

2.5 Degradation

In vitro degradation was evaluated from the calcium ion concentration and pH variation of the soaking medium (simulated body fluid, SBF; pH 7.4; 37± 0.5 ºC)[37] and weight loss of the scaffold. Ethylenediaminetetraacetic acid (EDTA) titration method was adopted to determine the calcium ion concentration in SBF as described elsewhere.[38] The weight loss of the uncoated and polymer coated PG/HA composite scaffolds was determined using SBF solution in a BOD incubator at 37 ± 0.5 ºC. Scaffolds were taken out at different time intervals, washed thoroughly with deionized water and dried in vacuum oven at 60 °C. Then the change in weight of the uncoated and polymer coated PG/HA composite scaffolds was measured. The percentage of weight loss was calculated using the following equation,

$$\text{Weight loss (\%)} = [(W_0 - W_t)/ W_0] \times 100$$

where, W_0 is the initial weight of the dried scaffolds and W_t is the final weight of the dried scaffolds. The pH variation during the degradation was assessed by immersing the scaffold in 30 ml of SBF solution in plastic containers with airtight lids at 37 ± 0.5 ºC and kept in an incubator without refreshing the media. At the end of predetermined incubation intervals, the medium of three samples per group were collected for the pH measurement. The values are expressed as the mean ± standard deviation (n=3). The variation in pH of the degradation medium (SBF solution) was measured every day during the dissolution study. The surface of the scaffolds after degradation study was examined using SEM.

2.6 Mechanical properties

The compressive strength of the scaffolds was calculated using a universal testing machine (3366, Instron® Co. Ltd. Norwood, MA, USA) at a crosshead speed of 1mm/min. The expression for the compressive strength S (in MPa) is given by the following equation:

$$S = F/A$$

where, F is the maximum compressive load (in newton), and A is the surface area (in mm^2) of the uncoated and polymer coated scaffolds perpendicular to the load axis (in square millimeters). The modulus of elasticity was measured from the slope of the stress-strain curve. The area under the stress-strain curve gives work of fracture of the pristine and polymer coated scaffolds.

2.7 Cytocompatibility

The cytotoxicity test was done for PG/HA composite and polymer coated PG/HA composite scaffolds with the osteoblast-like human osteosarcoma cell line (MG-63) grown in Eagles Minimum Essential Medium containing 10% fetal bovine serum (FBS) with 100 U ml^{-1} penicillin/streptomycin. The cells were maintained at 37 °C in 5% CO_2, 95% air and 100% relative humidity. Maintained cultures were passaged every week, and the culture medium was changed twice a week. The monolayer cells were detached with trypsin - EDTA to make single cell suspensions and viable cells were counted using a hemocytometer and diluted with medium containing 5% FBS to give final density of $1x10^5$ cells ml^{-1}. 100 µl per well of cell suspension were seeded into 96-well plates at plating density of 10,000 cells/well and incubated at 37 °C in

5% CO_2, 95% air and 100% relative humidity. After 24 h incubation, samples PG/HA and polymer coated PG/HA composite scaffolds in the form of powder were added to the culture medium at varying dosages 12.5, 25, 50, 100 and 200 µg ml^{-1}. Before adding, the samples were sterilized by immersing in 70% ethanol for 2 h and were then washed with phosphate buffered saline (PBS) solution. Aliquots of 100 µl of these different sample dilutions were added to the appropriate wells already containing 100 µl of medium with and without cells (blank), resulting in the required final sample concentrations. The medium without composite scaffold served as positive control. The plates were further incubated for 48 h at 37 °C in 5% CO_2, 95% air and 100% relative humidity. The assay was performed in triplicate.

After 48 h of incubation, 15 µl of 3-[4,5-dimethylthiazol-2-yl]2,5-diphenyltetrazolium bromide (MTT) (5 mg ml^{-1}) in PBS was added to each well and incubated at 37 °C for 4 h. The medium with MTT was then flicked off and the formazan crystals were solubilized in 100 µl of DMSO and measured the absorbance at 570 nm using micro plate reader. The percentage of cell viability was then calculated with respect to control as follows,

Cell viability (%) = [OD] Test / [OD] Control x 100

2.8 DAPI staining

After 0, 48 and 72 h of incubation, MG-63 cultured on PG/HA composite and G-PG/HA composite scaffolds were washed twice with PBS. The cells were fixed with fresh 4% paraformaldehyde in PBS for 15 min at room temperature. Then the samples were permeabilised with 0.5% Triton X-100 (in PBS) for 5 min. 4',6' diamino-2-phenylindole (DAPI; Invitrogen, Carlsbad, CA, USA) was used to stain DNA in nuclei. The scaffolds were sterilized using 10% FBS (in PBS) for 1 h, washed with PBS, stained with 50 µl DAPI (in PBS) and incubated in dark for 5 min. The scaffolds were examined under fluorescent microscope (EVOS FL from Life technologies), after repeated washing with PBS.

2.9 Statistical analysis

Statistical analyses were performed using SPSS (Statistical Package for the Social Sciences version 16, SPSS Inc., USA). Each quantitative data were obtained in triplicate from the

samples. Results are expressed as means ± standard deviation (SD). Student's t-test was used to compare among different samples with significance considered at 0.05 levels.

3. RESULTS AND DISCUSSION

3.1 Phase identification

Fig. 1 shows PXRD patterns of the HA, PG and HA/PG composite. The PG sample does not show any crystalline nature instead a broad peak is observed thus confirming the amorphous nature of the as prepared glass. Comparison of the XRD pattern of HA sample with JCPDS file for HA (09-0432) revealed that the unique crystalline phase of the sample to be HA. The crystallite size of the synthesized HA was calculated using Debye–Scherrer approximation and is about 24 nm. In the case of PG/HA composite scaffold, it was sintered at 600 ºC and hence, HA is observed as the major phase with tromelite ($Ca_4P_6O_{19}$) and α-calcium pyrophosphate (α-$Ca_2P_2O_7$) as the minor phases. The broad peak observed in the 2θ range 25 to 35 degree in PG/HA composite scaffold suggests the presence of nano-sized HA crystals and the less crystalline nature of the sample.

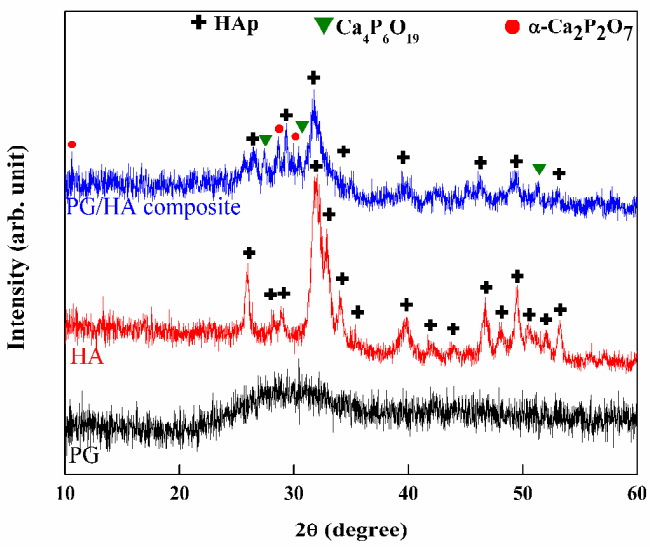

Fig. 1 XRD pattern of PG, HA and PG/HA composite sample.

3.2 FTIR analysis

FTIR spectra of PG/HA and polymer coated PG/HA composite scaffolds are shown in Fig. 2. The symmetric stretching vibrations of PO_3^{2-} of the phosphate group of PG are observed at 569,

726, 878 and 1092 cm^{-1} in the PG/HA composite scaffolds. The characteristic ν_4 vibrations of PO_4^{3-} of HA are found at 565 and 602 cm^{-1} along with the other ν_1, ν_2 and ν_3 phosphate peaks at 477, 961 and 1014 cm^{-1} respectively. The bands at 3571 and 631 cm^{-1} are the characteristic OH^- vibrations of HA. The peaks present at 878, 1414 and 1454 cm^{-1} are attributed to the carbonate impurities in the samples which are due to the adsorbed carbon dioxide from the atmosphere. Existence of PO_4^{3-}, OH^- and PO_3^{2-} vibrations in the scaffolds confirm the presence of HA and PG.[25]

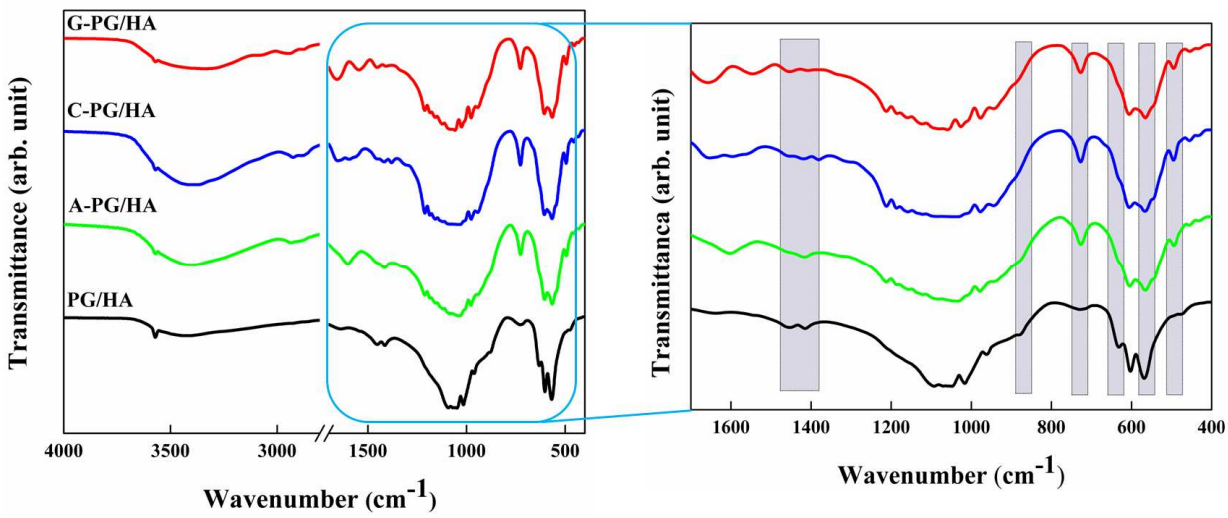

Fig. 2 FTIR spectra of PG/HA and polymer coated PG/HA composite scaffolds.

The FTIR spectrum of A-PG/HA composite scaffold is found to contain additional peaks at 1415 and 1602 cm^{-1} which are assigned to the $-COO^-$ stretching mode of alginate.[39-40] In the case of C-PG/HA composite scaffold, the peak at 1034 cm^{-1} can be ascribed to the C–O stretching vibration of the chitosan.[41] The peaks at 1652, 1596 and 1312 cm^{-1} are assigned to the N–H bending of the amide groups I and II of chitosan, respectively. The C-H bending and stretching vibrations of chitosan appeared at 1418 and 2923 cm^{-1}.[42] The peak observed at 1378 cm^{-1} is assigned to the acetamide groups, which corroborated with incomplete deacetylation of chitosan. The stretching vibrational peak of C=O at 1657 cm^{-1} (amide I), N–H bond at 1545 cm^{-1} (amide II) and C-N & N-H stretching at 1212 cm^{-1} (amide I) are attributed to the presence of gelatin in the G-PG/HA composite scaffold.[43] The peak at 1453 cm^{-1} is attributed to the aldimine group of glutaraldehyde used for crosslinking gelatin.

The interaction between the ceramic and polymer is well established as follows. The resolution of the characteristic doublet ν_4 PO_4^{3-} peaks of HA decreased with polymer coating. The ν_3 phosphate peak of HA at 1014 cm^{-1} disappeared in A-PG/HA, C-PG/HA and shifted to 1026 cm^{-1} in the case of G-PG/HA. The characteristic OH peak of HA at 631 cm^{-1} almost disappeared and the one at 3571 cm^{-1} decreased in intensity in the case of polymer coated samples. Intensity of the carbonate peaks at 1414 and 1454 cm^{-1} decreased. The peaks at 878 and 1092 cm^{-1} of PG disappeared and the peak at 726 cm^{-1} becomes well pronounced when coated with polymers.

3.3 Thermogravimetric analysis (TGA)

Polymer coating on the surface of the PG/HA composite scaffolds was further confirmed by means of thermal analysis. Fig. 3 shows the TGA plots of PG/HA composite and polymer coated PG/HA composite scaffolds. The PG/HA composite scaffold exhibits two distinct stages of weight losses as seen in the Fig. 3a. The first stage of weight loss of around 0.35% between 27 - 173 ºC attributed to the loss of adsorbed water molecules. The second stage occurs in the temperature range 173 – 800 ºC with weight loss of around 0.76%. This may be due to the gradual dehydroxylation of HA phase.

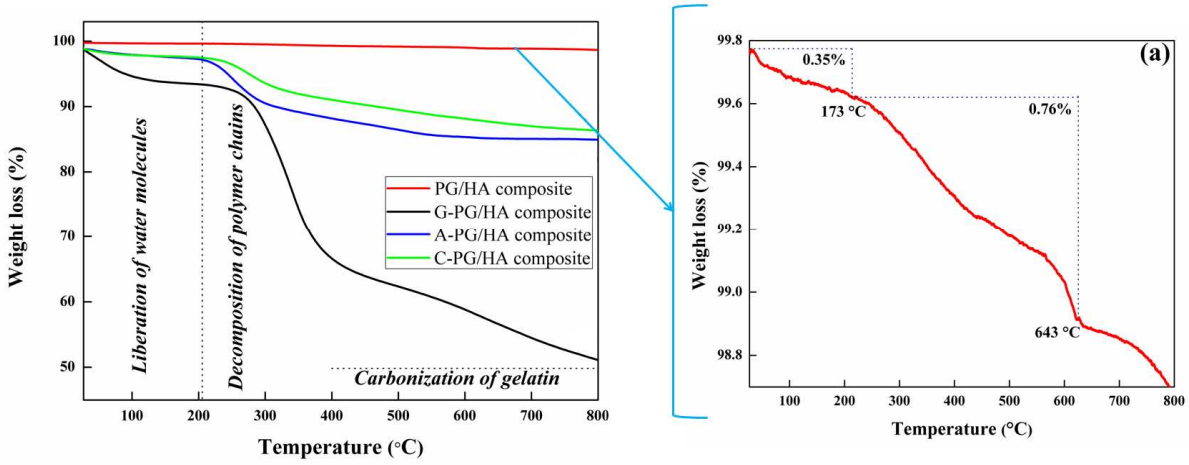

Fig. 3 TGA analysis of powdered composite scaffold and polymer coated composite scaffolds.

A-PG/HA and C-PG/HA composite scaffolds reveal two different weight losses. The first weight loss of around 3.01% and 2.6% is observed respectively for A-PG/HA and C-PG/HA in

the temperature range 27 - 210 ºC which is ascribed to the liberation of water content. The second weight loss occurred between 210 - 800 ºC for A-PG/HA (~ 8.99%) is mainly due to the decomposition of alginate, whereas the weight loss occurred in this range for C-PG/HA (~ 8.93%) is due to the processes like the dehydration of the polysaccharide rings and the decomposition of the acetylated and deacetylated units of chitosan.

In the case of G-PG/HA composite scaffold, the weight loss is found to occur in three different stages. As in the case of other scaffolds the first stage of weight loss of around 6.66% between 27 - 210 ºC is mainly due to the loss of adsorbed water molecules. The weight loss of 28.67% observed in the second stage between 210 - 400 ºC is corroborated with the decomposition of the polymeric chains of gelatin. The next stage of weight loss of about 12.45% occurred between 400 - 800 °C is attributed to the carbonation of the polymeric material. The overall weight loss at 800 ºC was found to be 1.11 wt%, 47.9 wt%, 13.87 wt% and 12.67 wt% for PG/HA, G-PG/HA composite, A-PG/HA composite and C-PG/HA composite scaffolds, respectively.

3.4 Microstructure of the composite scaffolds

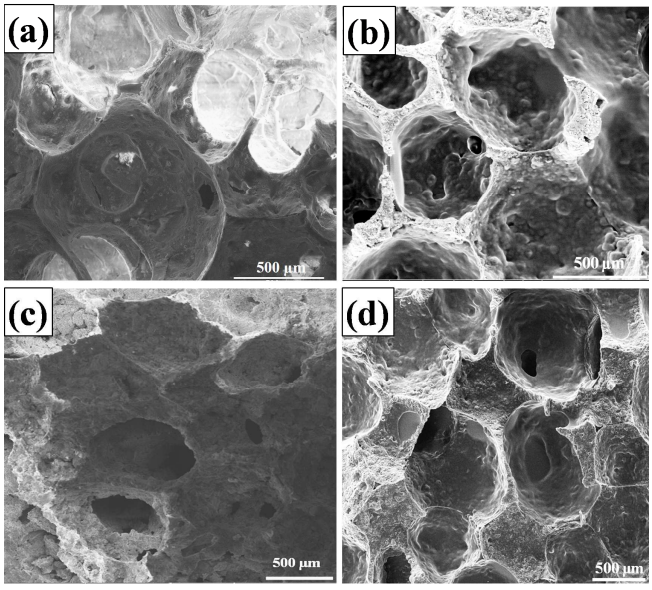

Fig. 4 SEM images of the composite scaffold microstructure for (a) PG/HA, (b) A-PG/HA (c) C-PG/HA and (d) G-PG/HA.

The microstructure of the scaffolds are shown in Fig. 4. The microstructure of the PG/HA composite scaffold as seen from the SEM images indicates that the foam structure is preserved (Fig. 4a) with completely interconnected pore system having pore diameter of ~200 - 500 µm. Polymer coating of the scaffold resulted in denser and smooth surfaced struts without cracks (Fig. 4b-4d), while preserving the porosity with interconnectivity and the similar structure have been reported by the foam replica method.[44-47] All composite scaffolds exhibit pore sizes higher than 100 µm, as generally required for tissue engineering applications.[48-49]

3.5 Porosity of the composite scaffolds

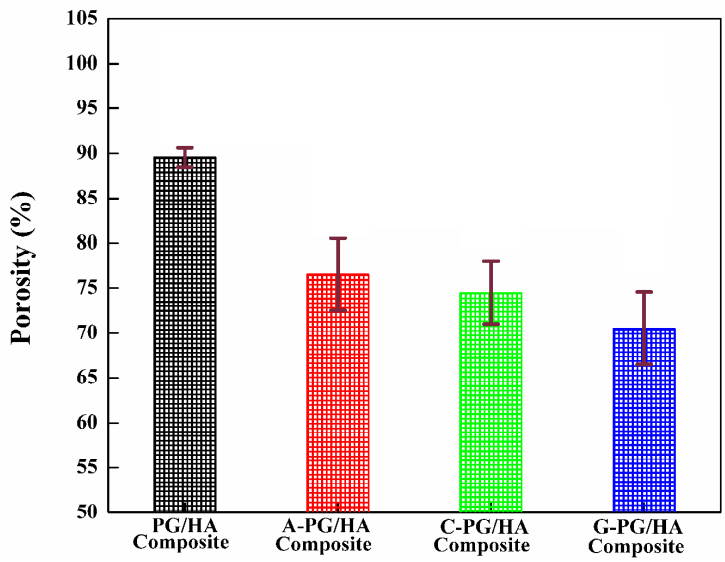

Fig. 5 Porosity of PG/HA composite and polymer coated PG/HA composite scaffolds.

In tissue engineering, porosity of the scaffold is very important for cell adhesion, proliferation, migration and ultimately for the formation of new tissue.[50] Moreover, elevated degree of porosity is necessary to allow fast vascularization of the bone graft.[51] Usually interconnectivity of the pores with a mean diameter of 100 µm or higher and open porosity greater than 50% are generally considered to be the minimum requirements for cell growth in the bioceramic scaffolds.[52-53] The porosity of the PG/HA, A-PG/HA, C-PG/HA and G-PG/HA composite scaffolds were determined to be ~89%, ~76%, ~74% and ~70% respectively (Fig. 5). All the scaffolds studied exhibits porosity above 50% satisfying the minimum requirements for tissue engineering applications. The reduced porosity of G-PG/HA composite scaffold may be due to

high concentration of gelatin coated. The observed porosity above 50% and pore sizes of the order of 200 μm and greater, from the SEM images discussed above, indicate that these composite scaffolds can be useful for tissue engineering applications.[48-49]

3.6 Degradation

Appropriate scaffold degradation is an important factor for better bone regeneration in bone tissue engineering.[54] The changes in calcium ion concentration observed in SBF solution as a function of soaking time for the scaffolds is given in Fig. 6a. Ca^{2+} ion concentration increases steeply until the 3rd day and it decreases gradually until the 18th day and thereafter it remains almost constant. Higher value of Ca^{2+} ion release from A-PG/HA is due to the Ca^{2+} ions present in alginate which was used for crosslinking the polymer. Next to A-PG/HA composite scaffold, pristine PG/HA composite scaffold is the one which released higher Ca^{2+} ion. The dealkalization process due to the direct contact of PG/HA composite scaffold with the medium is responsible for this. Less Ca^{2+} ion release was observed from gelatin coated one and the least from the chitosan coated scaffold. The polymer coating prevents the direct contact of the medium with the ceramic surface and thereby reducing the dissolution. This decrease in Ca^{2+} ion may be due to the precipitation of apatite from SBF on the surface of scaffolds.[55-56] SEM image of the surface of the scaffold after degradation study is shown in Fig. 7. Though there is possibility of apatite deposition as suggested from the decrease in Ca^{2+} ion concentration the apatite deposition is not significant enough to be observed on the surface except in the case of A-PG/HA in which there are few deposits observed due to the enhanced Ca^{2+} ions that leached from the polymer coating. Significant apatite deposition is observed when the soaking medium is periodically replenished.[57]

The weight loss of PG/HA and polymer coated PG/HA composite scaffolds with incubation in SBF until 28th day is shown in Fig. 6b. The order of weight loss is found to be G-PG/HA > A-PG/HA > C-PG/HA > PG/HA. Weight loss is very significant in gelatin coated scaffold when compared to other scaffolds. The weight losses of PG/HA composite and A-PG/HA composite scaffolds gently increased up to 12th day whereas in the case of C-PG/HA and G-PG/HA composite scaffolds the increase was up to 15th day. This order corresponds to the weight loss observed in the thermal analysis. Hence the loss of weight can be ascribed to the degradation of polymer coating over the scaffold. The predominant degradation of G-PG/HA

composite scaffold can be ascribed to the hydrophilic nature of the gelatin polymer which leads to quick hydrolysis of the macromolecular chains.[58] The weight loss of A-PG/HA composite scaffold depend on the molecular weight, chemical structure and crosslinking cations. The degradation of alginate can be explained in terms of ion exchange between Ca^{2+} and Na^{+} i.e. Na^{+} ions replaced Ca^{2+} and bonded with carboxylic groups in alginate.[59-61] The weight loss of C-PG/HA composite scaffold is attributed to its degradability by hydrolysis of the glycosidic bonds in the chitosan polymer.[62] The less weight loss of chitosan than alginate is due to the high charge density of chitosan polymer.[63-64] Weight loss of the polymer coated PG/HA composite scaffolds resulted not only from degradation of the polymer coating but also from dissolution of the ceramic composite during immersion in SBF. After 12^{th} day up to 28^{th} day no significant weight loss was observed except slight reduction in weight loss for all the composite scaffolds this indicates the termination of scaffold degradation as the medium was not replaced with fresh solution. In *in vivo* environment there will be a constant circulation of body fluid that can lead to the degradation of the scaffold, apatite deposition over the scaffold and further cellular activities.

The pH variation of the soaking medium during the dissolution study is shown in Fig. 6c. pH value of all the composite scaffold soaked media increased up to 6 days due to the increase in OH^{-} ions. After 6^{th} day up to 18^{th} day, pH value rapidly decreased which is assumed to be due to the deposition of apatite that consumes OH^{-} ions. But the apatite deposition was not so significant enough to be observed except in the case of A-PG/HA as mentioned earlier due to the lack of replenishment of the medium.

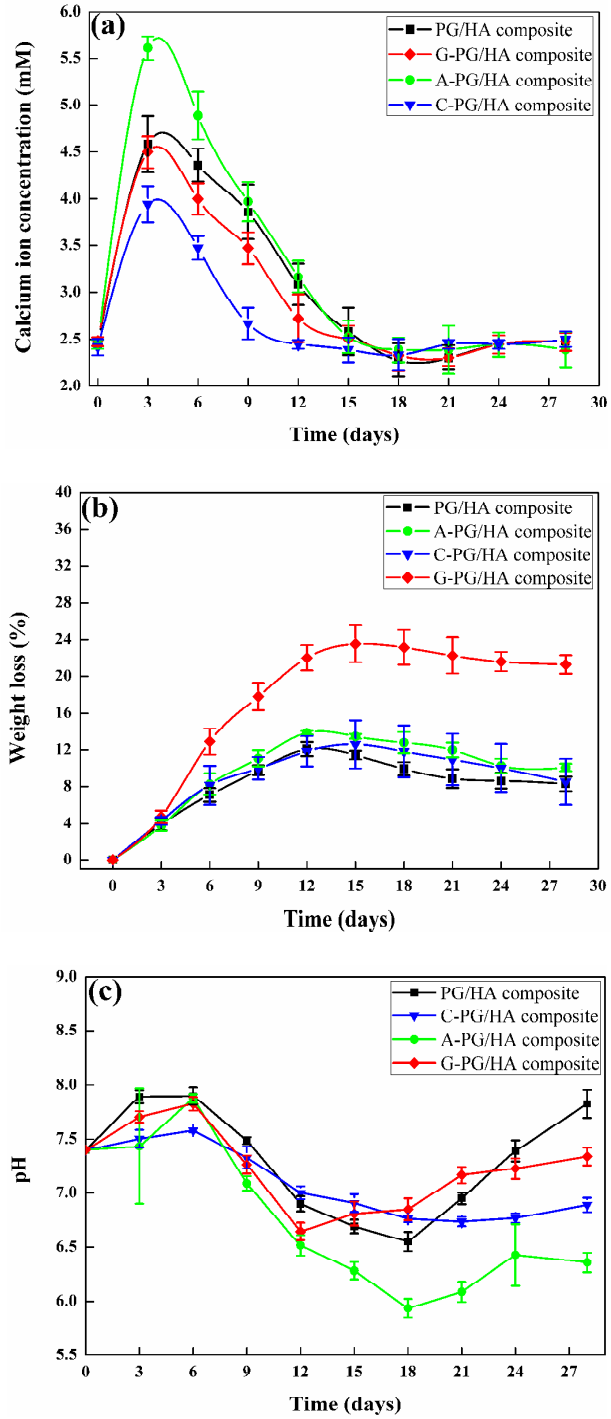

Fig. 6 (a) Ca^{2+} ion concentration of the soaking medium (b) weight loss of the scaffold and (c) pH variation of the soaking medium during degradation studies.

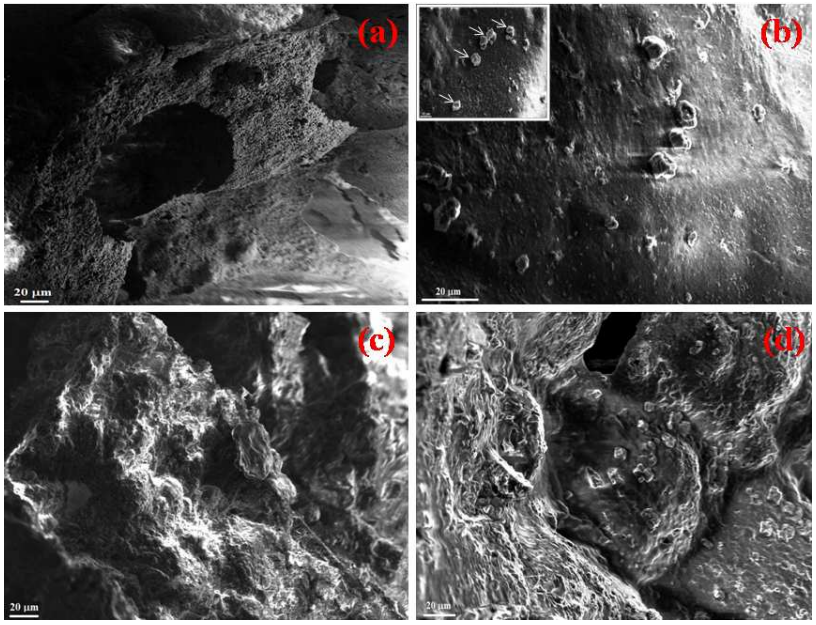

Fig. 7 SEM images of (a) PG/HA, (b) A-PG/HA, (c) C-PG/HA and (d) G-PG/HA composite scaffolds after degradation analysis.

3.7 Mechanical properties

Indeed polymer coating is considered to be a smart approach for fabricating tough, highly porous and mechanically strong scaffolds of highly brittle ceramics. Typical stress-strain curve of PG/HA composite and polymer coated PG/HA composite scaffolds are shown in Fig. 8. Up to 40% strain, all composite scaffolds illustrated two stages, a maximum stress stage with a positive slope followed by a plateau stage created through the brittle crushing of the struts, causing an apparent stress drop. In particular, positive stress stage was observed in the range of 2 – 6% strain for PG/HA, A-PG/HA and C-PG/HA composite scaffolds while for G-PG/HA composite the range extended up to ~ 15% strain. For PG/HA, A-PG/HA and C-PG/HA composite scaffolds it could be observed by reducing the full scale of Y-axis as shown in the inset of Fig.8a. Gelatin coated PG/HA composite scaffold exhibits significantly enhanced mechanical properties than PG/HA and other polymer coated PG/HA composite scaffolds and it provides more stable stress-strain curve. The elastic modulus of the scaffold should be analogous to tissue to be treated in order to minimize stress shielding which will reduce the problems of bone resorption.[65] The elastic modulus of the G-PG/HA composite scaffold (0.0183 GPa) is significantly greater than for the other composite scaffolds. The area under the stress–strain curve represents the work of

fracture and enumerates the ability of a scaffold to resist fracture. The work of fracture of the PG/HA, A-PG/HA, C-PG/HA and G-PG/HA composite scaffolds are 0.1825 kJm^{-3}, 1.081 kJm^{-3}, 0.8525 kJm^{-3} and 18.125 kJm^{-3}, respectively. It is clear that gelatin coating on the ceramic scaffold significantly increases the work of fracture of the scaffold.

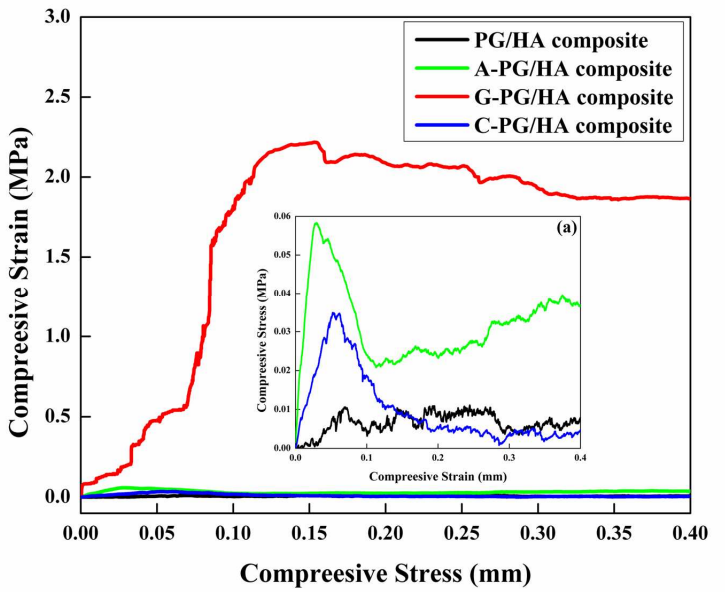

Fig. 8 Stress-strain curve of PG/HA and polymer coated PG/HA composite scaffolds.

Fig. 9 shows the compressive strength of the PG/HA and polymer coated PG/HA composite scaffolds. The compressive strength is estimated to be 0.03 ± 0.02, 2.22 ± 0.42, 0.13 ± 0.04, and 0.13 ± 0.01 MPa respectively for PG/HA, G-PG/HA, A-PG/HA and C-PG/HA composite scaffolds. It demonstrates that the compressive strength increases when coated with polymers. Alginate and chitosan coating did not improve the compressive strength significantly but gelatin coating increased the compressive strength 7 times to that of PG/HA composite scaffold. Correspondingly all the scaffolds crushed into powder except the G-PG/HA composite during the compressive strength test which indicates that the high elasticity of gelatin polymer is responsible for the high compressive strength of the scaffold.

Compressive strength always depends on porosity and it increases with decrease in porosity value of the scaffold. The improved mechanical strength of the polymer coated PG/HA composite scaffold is explained by the micron-scale crack-bridging mechanism.[66] The polymeric coating covers the space between the microcracks in the struts, forming continuous bridges

which enhances the structural integrity of the scaffolds and lead to a toughening effect. The high content of gelatin infiltrated into the scaffold gets filled in the micropores and the microcracks of the struts and thereby makes the weak and brittle struts to become stronger and tougher while enhancing the mechanical stability. In general, the compressive strength of cancellous bone is in the range of 0.2–4MPa when the relative density is about 0.1.[67] As the compressive strength of the G-PG/HA composite scaffold falls closer to the higher limit of the above said range, it can be handled safely by cell biologists and surgeons.[34] It is to be mentioned here that a similar result was observed for gelatin coated bioceramic scaffolds with two to four times enhanced compressive strength.[28]

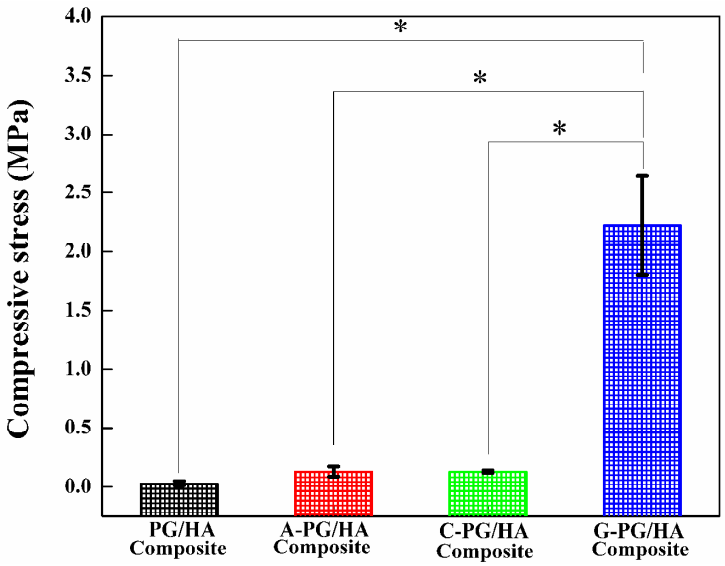

Fig. 9 Compressive strength of uncoated and polymer coated composite scaffolds. * is statistically significant difference ($P < 0.05$).

3.8 *In vitro* biocompatibility

MTT assay is a quick method to evaluate the cell-material interaction as an initial biocompatibility test before proceeding *in vivo*. The assay is based on the reduction of yellow colored MTT into insoluble violet color formazan crystals by the mitochondria of living cells.[68] The biocompatibility assessment has been performed by measuring the viability of human osteoblast-like MG-63 cells cultured on different concentrations of PG/HA composite and polymer (alginate, chitosan and gelatin) coated PG/HA composite scaffolds and the result is given in Fig. 10. It was observed that the PG/HA composite and polymer coated PG/HA

composite scaffolds did not show any adverse effects up to 200 µg/ml and were biocompatible towards MG-63 cells with no statistically significant difference ($P < 0.05$). The better cell viability may be due to the presence of calcium phosphate or Ca^{2+} in the composite scaffolds.[69-70] Optical images of MG-63 cells and cells containing various concentrations of the PG/HA and polymer coated PG/HA composite scaffolds incubated for 48 h are shown in Fig. 11. According to ISO 10993 - 5: 2009, PG/HA and polymer coated PG/HA composite scaffolds revealed cell viability greater than 70% indicating that all the samples are non toxic with human osteoblast-like MG-63 cells which reveals their biocompatibility.

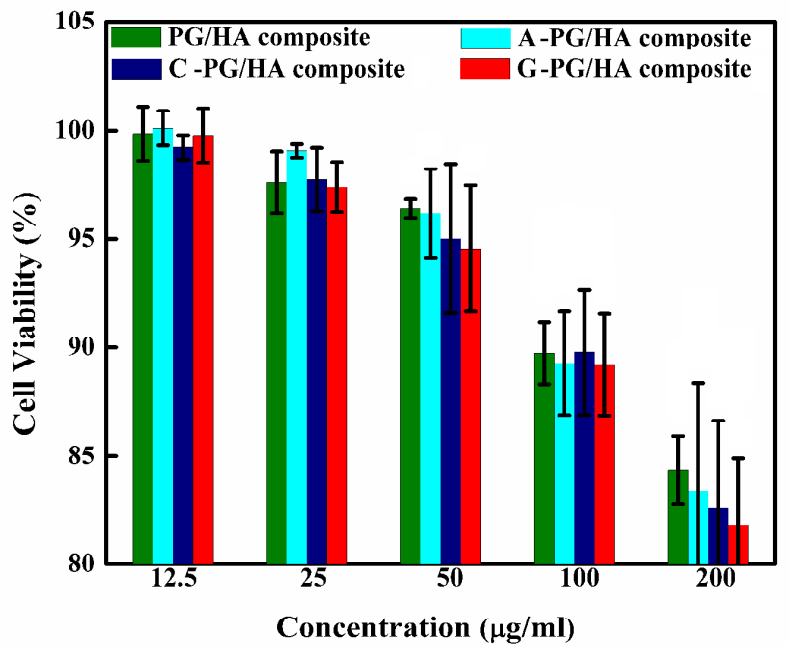

Fig. 10 Biocompatability of PG/HA composite scaffold and polymer coated PG/HA composite scaffolds with MG-63 cells. Values reported are mean ± standard deviation (SD), n=3.

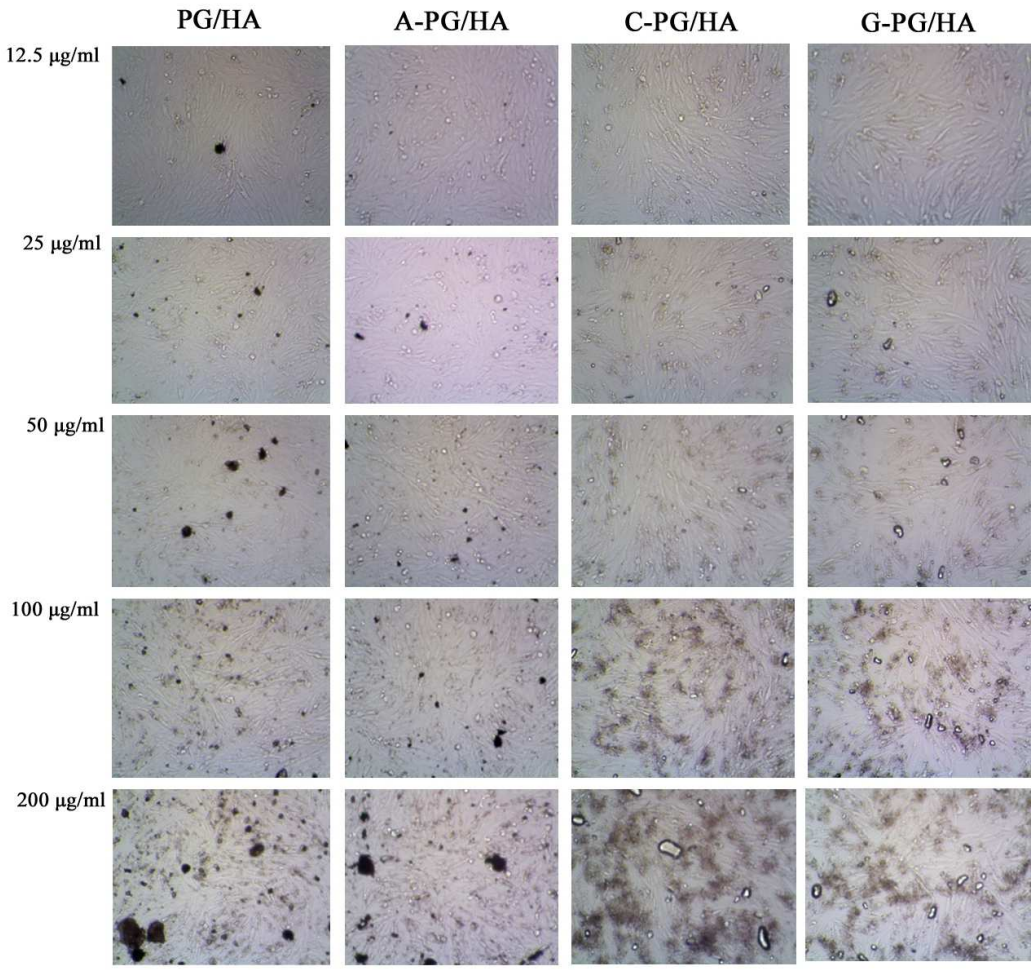

Fig. 11 Optical microscope images of MG-63 cells on PG/HA composite scaffold and polymer coated PG/HA composite scaffolds for different concentration of samples.

3.9 DAPI staining

The cellular uptake of the PG/HA composite and G-PG/HA composite scaffolds with MG-63 cells was examined *via* DAPI staining. Two different concentrations *viz.,* 2 and 4 mg were treated with cells for 0, 48 and 72 h incubation. Then fluorescence microscopic images were recorded after DAPI staining of the cell nuclei. Initially there was no significant difference in cell population as observed in PG/HA composite and G-PG/HA composite scaffolds which is similar to the control sample (Fig. 12a). After 48 h, cells attached to PG/HA composite and G-PG/HA composite (Fig. 12b) and the cell population got significantly increased. Further, observation at 72 h confirmed that the cells attached and proliferated on the composite scaffold in a manner

similar to the control sample (Fig. 12c). However, cell attachment was found to decrease with increasing dosage of the composite sample. On other hand, more cells were found to be attached to the less concentration composite scaffolds than higher concentration but are comparable to the control sample.

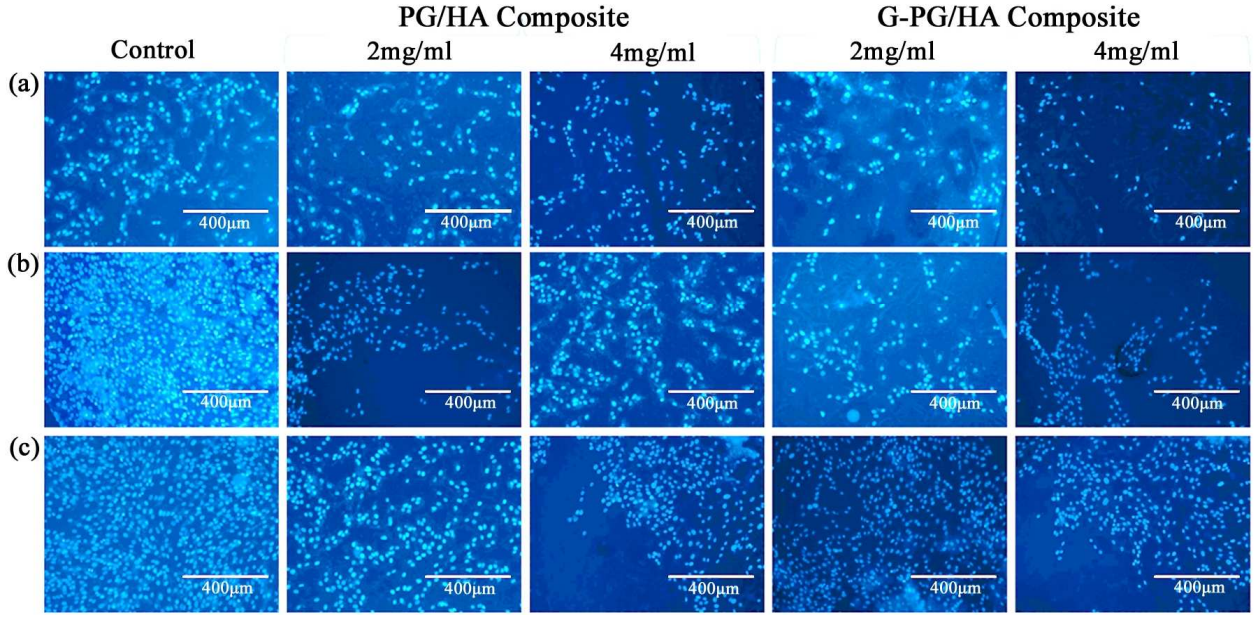

Fig. 12 Fluorescence microscope images for DAPI staining of PG/HA composite and G-PG/HA composite scaffolds with MG-63 cells for (a) 0, (b) 48 and (c) 72 h.

4. CONCLUSIONS

Biodegradable, three dimensional, highly porous PG/HA composite scaffold were prepared by polymer foam replication method. This ceramic composite scaffold was coated with alginate, chitosan and gelatin in order to improve the mechanical strength. Further analysis revealed that polymer coating did not affect the pore interconnectivity but significant porosity alteration was observed. Biodegradation studies demonstrated that all the composite scaffolds have degraded significantly. Among the three polymers alginate, chitosan and gelatin studied, gelatin coating on PG/HA scaffold exhibit enhanced mechanical strength and it did not affect the biocompatibility of the scaffold. The addition of a polymer over the porous bioceramic scaffold not only boosts the mechanical properties of the ceramic scaffold but also allows the functionalization of the scaffold surface. The present investigation and results clearly indicate that the G-PG/HA

composite scaffold material is a promising candidate for its application in bone tissue engineering than PG/HA composite and other polymer coated composite scaffolds.

ACKNOWLEDGMENTS

This work was financially supported by University Grants Commission, India through the project (Project Ref. no. 41-1013/2012 SR). We thank Dr. A. Thamizhavel of TIFR for a critical reading of the manuscript.

REFERENCES

1 http://www.boneandjointdecade.org/default.aspx?contId=229.

2 http://www.boneandjointburden.org/.

3 http://osha.europa.eu/en/topics/msds/facts_html.

4 V. Karageorgiou and D. Kaplan, *Biomaterials,* 2005, **26**, 5474–5491.

5 T. Kokubo and H. Takadama, *Biomaterials,* 2006, **27**, 2907–2915.

6 R. Akbarzadeh and A. M. Yousefi, *J*, *Biomed. Mater. Res. Part B,* 2014, **102B**, 1304–1315.

7 Y. X. Huang, J. Ren, C. Chen, T. B. Ren, and X. Y. Zhou, *J. Biomater. Appl.,* 2008**, 22**, 409-432.

8 H. H. Lu, S. F. El-Amin, K. D. Scott and C. T. Laurencin, *J Biomed. Mater. Res. A,* 2003, **64A**, 465–74.

9 A. Zamanian, S. Farhangdoust, M. Yasaei, M. Khorami and M. Hafezi, M, *Int. J. Appl. Ceram. Technol.,* 2014, **11**, 12–21.

10 A. Clark, T. A. Milbrandt, J. Z. Hilt and D.A. Puleo, *J. Biomed. Mater. Res. Part A,* 2014, **102A**, 348–357.

11 S.S. Kim, K.M. Ahn, M.S. Park, J.H. Lee, C.Y. Choi and B.S. Kim, *J. Biomed. Mater. Res. A,* 2007, **80A**, 206–215.

12 M. Mozafari and F. Moztarzadeh, *Ceram. Int.,* 2014, **40**, 5349-5355.

13 Y. Zhou, S. Fu, Y. Pu, S. Pan and A. J. Ragauskas, *Carbohydrat. Polym.,* 2014, **112**, 277–283.

14 M. Jafarkhani, A. Fazlali, F. Moztarzadeh, Z. Moztarzadeh and M. Mozafari, *Ind. Eng. Chem. Res*., 2012, **51**, 9241−9249.

15 L. Estevez, A. Kelarakis, Q. Gong, E. H. Daas and E. P. Giannelis, *J. Am. Chem. Soc*., 2011, **133**, 6122–6125.

16 Q. Fu, M. N. Rahaman, F. Dogan and B. S. Bal, *Biomed. Mater.,* 2008, **3**, 025005-025012.

17 W. Lia, P. Nooeaida, A. R. Roetherb, D. W. Schubertb and A. R. Boccaccini, *J. Eur. Ceram*. *Soc*., 2014, **34**, 505-514.

18 O. Bretcanu, F. Baino, E. Verné and C. Vitale-Brovarone, *J. Biomater. App.,* 2014**, 28**, 1287-1303.

19 Q. Chen, D. Mohn and W.J. Stark, *J. Am. Ceram. Soc.,* 2011, **94**, 4184–4190.

20 A. Hoppe, B. Jokic, D. Janackovic, F. Fey, P. Greil, S. Romeis, J. Schmidt, W. Peukert, J. Lao, E. Jallot and A. R. Boccaccini, *ACS Appl. Mater. Interfaces,* 2014, **6**, 2865–2877.

21 K. C. R. Kolan, M. C. Leu, G. E. Hilmas, R. F. Brown and M. Velez, *Biofabrication,* 2011, **3**, 025004-025013.

22 D.M. Yunos, O. Bretcanu and A.R. Boccaccini, *J. Mater. Sci.*, 2008, **43,** 4433–4442.

23 M. Peroglio, L. Gremillard, J. Chevalier, L. Chazeau, C. Gauthier and T. Hamaide, *J. Eur. Ceram. Soc.*, 2007, **27,** 2679–2685.

24 L Hench and J. Jones, *Biomaterials, Artificial Organs and Tissue Engineering*, Woodhead Publishing Limited, Cambridge, UK, 2005

25 R. Govindan and E. K. Girija, *J. Mater. Chem., B* 2014, **2**, 5468-5477.

26 Q. Z. Chen and A. R. Boccaccini, *J. Biomed*. *Mater*. *Res*. 2006, **77A**, 445–457.

27 J. Hum, K.W. Luczynski, P. Nooeaid, P. Newby, O. Lahayne, C. Hellmich and A. R. Boccaccini, *Strain,* 2013, **49**, 431–439.

28 A. L. Metze, A. Grimm, P. Nooeaid, J. A. Roether, J. Hum,P.J. Newby, D. W. Schubert and A. R. Boccaccini, *Key Eng. Mater.,* 2013, **541**, 31–39.

29 D. Meng, L. Francis, I. D. Thompson, C. Mierke, H. Huebner, A. Amtmann, I. Roy and A. R. Boccaccini, *J. Mater. Sci: Mater. Med.,* 2013, **24**, 2809–2817.

30 A. M. Vega, T. Gómez-Quintero, R. Nuñez-Anita, L. Acosta-Torres and V. Castaño, *J. Nanotechnology,* 2012, **2012**, 1-10.

31 *Biomedical materials*, ed. R. Narayan, Springer, Bosten, US, 2009.

32 *Natural and Synthetic polymers,* ed. S. G. Kumbar, C. T. Laurencin and M. Deng, Elsevier, San Diego, USA, 2014.

33 A. Philippart, A. R Boccaccini, C. Fleck, D. W. Schubert and J. A. Roether, *Expert Rev*. *Med*. *Devices* 2015, **12**, 93–111.

34 Q. Z. Chen, I. D. Thompson and A. R. Boccaccini, *Biomaterials,* 2006, **27**, 2414-2425.

35 J. Xu, X. Zhou, H. Ge, H. Xu, J. He, Z. Hao and X. Jiang, *J. Biomed. Mater. Res. A*, 2008, **87A**, 819-824.

36 D. Deborah, W. Li, J. A. Roether, D. W. Schubert, M. C. Crovace, A. C. M. Rodrigues, E. D. Zanotto and A. R. Boccaccini, *Sci. Technol. Adv. Mater.,* 2013, *14*, 045008-045018.

37 A. C. Tas, *Biomaterials,* 2000, **21**, 1429–1438.

38 G. Suresh Kumar, A. Thamizhavel, Y. Yokogawa, S. N. Kalkura and E. K. Girija, *Mater. Chem. Phys.* 2012, **134**, 1127-1135.

39 E. Torres, Y. N. Meta, M. L. Blazquez, J. A. Munoz, F. Gonzalez and A. Ballester, *Langmuir* 2005, **21**, 7951-7958.

40 K. Sangeetha , A. Thamizhavel and E. K. Girija, *Mater. Lett.* 2013, **91**, 27-30.

41 A. Shavandi, A. A. Bekhit, Z. Sun , A. Ali and M. Gould, *Mater. Sci. Eng. C* 2015, **55,** 373–383.

42 C. E. Tanase, M. I. Popa and L. Verestiuc, *Mater. Lett.* 2011, **65**, 1681–1683.

43 J. Xu, J. Yan, Q. Gu, J. Li and H. Wang, *Mater. Lett.* 2011, **65,** 2404–2406.

44 M. M. Erol, V. Mourino, P. Newby, X. Chatzistavrou, J. A. Roether, L. Hupa and A. R. Boccaccini, *Acta Biomater.,* 2012, **8**, 792–801.

45 F. Baino and C. Vitale-Brovarone, *J. Biomed. Mater. Res. A,* 2011, **97**, 514–35.

46 V. Mourino, P. Newby and A. R. Boccaccini, *Adv. Eng. Mater.,* 2010, **12**, B283-B291.

47 P. Nooeaid, W. Li, J. A. Roether, V. Mourino, O. Goudouri, D. W. Schubert and A. R. Boccaccini, *Biointerphases,* 2014, **9**, 041001-041010.

48 L. C. Gerhardt and A. R. Boccaccini, *Materials,* 2010, **3**, 3867-3910.

49 V. Guarino, F. Causa and L. Ambrosio, *Expert Rev. Med. Dev.,* 2007, **4**, 405-418.

50 Y. Ikada, *J. R. Soc. Interface,* 2006, **3**, 589-601.

51 C. Vitale-Brovarone, M. Miola, C. Balagna and E. Verne, *Chem. Eng. J.,* 2008, **137**, 129–136.

52 S. F. Hulbert, F. A. Young, R. S. Mathews, J. J. Klawitter, C. D. Talbert and F. H. Stelling, *J. Biomed. Mater. Res.,* 1970, **4**, 433–56.

53 J. O. Hollinger, J. Brekke, E. Gruskin and D. Lee, *Clin. Orthop. Relat. Res.* 1996, **324**, 55–65.

54 E. Alsberg, H. J. Kong, Y. Hirano, M. K. Smith, A. Albeiruti and D. J. Mooney, *J. Dent. Res.,* 2003, **82**, 903–908.

55 L. L. Hench, *J. Am. Ceram. Soc.,* 1991, **74**, 1487-1510.

56 S. W. Ha, R. Reber, K. L. Eckeret, M. Petitmermet, J. Mayer, E. Wintermantel, K. Baerlocher and H. Gruner, *J. Am. Ceram. Soc.,* 1998, **81**, 81-88.

57 G. Suresh Kumar, E. K. Girija, A. Thamizhavel, Y. Yokagawa and S. N. Kalkura, *J. Colloid. Interface Sci*., 2010, **349**, 56-62.

58 M. Peter, N.S. Binulal, S.V. Nair, N. Selvamurugan, H. Tamura and R. Jayakumar, *Chem. Eng. J.,* 2010, **158,** 353–361.

59 K. Y. Lee and D. J. Mooney, *Prog. Polym. Sci.,* 3011, **37**, 106–126.

60 P. Lertsutthiwong, P. Rojsitthisak, and U. Nimmannit, *Mater. Sci. Eng. C- Bio. S.,* 2009, **29**, 856–860.

61 L. S. Nair and C. T. Laurencin, *Prog. Polym. Sci.,* 2007, **32**, 762–798.

62 A. V. Il'ina, V. P. Varlamov, *Appl. Biochem. Micro.*, 2004, **40**, 300–303.

63 M. Lee, W. Li and R. K. Siu, *Biomaterials*, 2009, **30**, 6094–6101.

64 X. Z. Shu and K. J. Zhu, *Int. J. Pharm.*, 2000, **201**, 51–58.

65 H. M. Frost, *Bone* 1998, **23**, 395-398.

66 G. Pezzotti and S. M. F. Asmus, *Mater. Sci. Eng. A Struct. Mater*., 2001, **316**, 231-237.

67 L.J. Gibson and M. F. Ashby, *Cellular Solids: Structure and Properties*, Cambridge University Press, Cambridge, London, 1999.

68 T. Mosmann, *J. Immun. Meth.,* 1983, **65**, 55–63.

69 M. Wiens, X. Wang, U. Schlosssmacher, I. Lieberwirth, G. Glasser, H. Ushijima, H. C. Schröder and W. E. G. Müller, *Calcif. Tissue Int.,* 2010, **87**, 1–12.

70 S. Maeno, Y. Niki, H. Matsumoto, H. Morioka, T. Yatabe, A. Funayama, Y. Toyama, T. Taguchi and J. Tanaka, *Biomaterials,* 2005, **26**, 4847–4855.

Graphical Abstract

Biopolymer coated PG/HA composite scaffolds were prepared with enhanced mechanical properties for bone tissue engineering applications.